European Journal of Pharmacology 682 (2012) 73–78

Contents lists available at SciVerse ScienceDirect

European Journal of Pharmacology

journal homepage: www.elsevier.com/locate/ejphar

Neuropharmacology and Analgesia

Inhibitory effects of magnolol on voltage-gated Na^+ and K^+ channels of NG108-15 cells

Chi-Li Gong [a,1], Kar-Lok Wong [b,c,1], Ka-Shun Cheng [b,1], Chang-Shin Kuo [d], Chia-Chia Chao [d], Min-Fan Tsai [a], Yuk-Man Leung [d,*]

[a] Department of Physiology, China Medical University, Taichung 40402, Taiwan
[b] Department of Anesthesiology, China Medical University and Hospital, Taichung 40402, Taiwan
[c] Department of Anesthesiology, LKS Faculty of Medicine, University of Hong Kong, Hong Kong, China
[d] Graduate Institute of Neural and Cognitive Sciences, China Medical University, Taichung 40402, Taiwan

ARTICLE INFO

Article history:
Received 6 October 2011
Received in revised form 31 January 2012
Accepted 9 February 2012
Available online 21 February 2012

Keywords:
Magnolol
Voltage-gated Na^+ channel
Voltage-gated K^+ channel
Block
NG108-15 cell

ABSTRACT

Magnolol, a polyphenolic compound isolated from Houpu, a Chinese herb from the bark of *Magnolia officinalis*, has been reported to have *in vitro* and *in vivo* neuroprotective effects. In spite of these reported beneficial effects, studies on the direct impact of magnolol on neuronal ion channels have been scarce. Whether magnolol affects voltage-gated Na^+ channels (VGSC) and voltage-gated K^+ (Kv) channels is unknown. Using the whole-cell voltage-clamp method, we studied the effects of magnolol on voltage-gated ion channels in neuronal NG108-15 cells. Magnolol inhibited VGSC channels with mild state-dependence (IC_{50} of 15 and 30 μM, at holding potentials of −70 and −100 mV, respectively). No frequency-dependence was observed in magnolol block. Magnolol caused a left-shift of 18 mV in the steady-state inactivation curve but did not affect the voltage-dependence of activation. Magnolol inhibited Kv channels with an IC_{50} of 21 μM, and it caused a 20-mV left-shift in the steady-state inactivation curve without affecting the voltage-dependence of activation. In conclusion, magnolol is an inhibitor of both VGSC and Kv channels and these inhibitory effects may in part contribute to some of the reported neuroprotective effects of magnolol.

1. Introduction

Magnolol, a polyphenolic compound isolated from Houpu, a traditional Chinese herb from the bark of *Magnolia officinalis*, has been reported to have multiple pharmacological actions. Magnolol has anti-inflammatory effects, possibly via inhibitory actions against nuclear factor-κB (Mainardi et al., 2009). The antioxidative properties of magnolol have been proposed for treating dermatological disorders (Shen et al., 2010). Magnolol has been demonstrated to have anticancer effects in thyroid carcinoma cells (Huang et al., 2007), urinary bladder cancer cells (Lee et al., 2008) and glioblastoma cells (Chen et al., 2009). Protective effects of magnolol on the vasculature have been reported. For instance, a vasorelaxant action by magnolol in rat aorta has been reported; such an effect may be attributed to endothelial-derived relaxing factor release and magnolol blockade of voltage-gated Ca^{2+} channels in smooth muscle cells (Teng et al., 1990). In rats, magnolol has also been shown to offer protection against cerebral ischemic injury (Chang et al., 2003).

There have been reports of the beneficial effects of magnolol on neurons *in vitro* and the nervous system *in vivo*. Magnolol has been shown to have anxiolytic and anti-depressant effects in rodent models (Maruyama et al., 1998; Xu et al., 2008). Magnolol could protect mice from learning and memory impairment and neuronal loss due to aging (Matsui et al., 2005, 2009). Magnolol was shown to reduce inflammatory pain in mice, suggesting it is potentially an analgesic agent (Lin et al., 2007, 2009). Magnolol has also been demonstrated to have anti-convulsant effect via interacting with the GABA-benzodiazepine receptors (Chen et al., 2011) and the NMDA receptors (Lin et al., 2005). *In vitro* studies have shown that magnolol protects rat cortical neurons from chemical hypoxia induced by cyanide (Lee et al., 1998). In addition, magnolol could protect cerebellar granule cells from injury caused by glucose deprivation, hydrogen peroxide and excitotoxicity (Lin et al., 2006).

In spite of the reported beneficial effects of magnolol on neural tissues, studies on the direct impact of magnolol on neuronal ion channels have been scarce. In one study using fura-2 as fluorescent dye, it was shown that magnolol inhibits Ca^{2+} influx triggered by depolarization or glutamate in rat cerebellar granule cells (Lin et al., 2005). Voltage-gated Na^+ channels (VGSC) and voltage-gated K^+ (Kv) channels are directly involved in neuronal excitability (Hille, 2001). Whether magnolol affects VGSC and Kv channels is unknown. In the present study, we demonstrated that magnolol inhibited both VGSC and Kv channels in neuronal NG108-15 cells. NG108-15 cells were formed by fusion of mouse N18TG2 neuroblastoma cells with rat

* Corresponding author. Tel.: +886 4 22053366x2185; fax: +886 4 22076853.
E-mail address: ymleung@mail.cmu.edu.tw (Y.-M. Leung).
[1] These authors contributed equally to this work.

0014-2999/$ – see front matter © 2012 Elsevier B.V. All rights reserved.
doi:10.1016/j.ejphar.2012.02.013

C6-BU-1 glioma cells (Hamprecht et al., 1985). Magnolol also altered the gating of VGSC and Kv channels. These inhibitory effects may in part contribute to some of the reported neuroprotective effects of magnolol.

2. Materials and methods

2.1. Chemicals and cell culture

Magnolol and lidocaine were purchased from Sigma-Aldrich (St. Louis, MO), and were dissolved in DMSO at a stock concentration of 100 mM. NG108-15 cells were grown at 37 °C in 5% CO_2 in Dulbecco's modified Eagle's medium (DMEM) supplemented with 10% fetal bovine serum (Invitrogen, Carlsbad, CA) and penicillin-streptomycin (100 units/mL, 100 μg/mL) (Invitrogen).

2.2. Electrophysiology

Voltage-clamp experiments were performed as we previously described (Chou et al., 2009; Leung et al., 2010a, 2010b). NG108-15 cells were voltage-clamped in the whole-cell mode. Glass capillary tubes (OD 1.5 mm, ID 1.10 mm, Sutter Instrument, Novato, CA) were prepared with a micropipette puller (P-87, Sutter Instrument), and then polished by a microforge (Narishige Instruments, Inc., Sarasota, FL). The extracellular solution contained (mM): 140 NaCl, 4 KCl, 1 $MgCl_2$, 2 $CaCl_2$, 10 HEPES (pH 7.4 adjusted with NaOH). When Kv currents were measured, the pipette solution was composed of (mM): 140 KCl, 1 $MgCl_2$, 1 EGTA, 10 HEPES, and 5 MgATP (pH 7.25 adjusted with KOH). When Na^+ currents were measured, the pipette solution had (mM): 120 CsCl; 20 TEA-Cl; 8 NaCl; 1 $MgCl_2$; 1 EGTA; 10 HEPES and 5 MgATP (pH 7.25 adjusted with CsOH), and a Ca^{2+}-free extracellular solution with 20 μM EGTA supplementation was used. The resistance of the pipettes was from 3 to 6 MΩ. The currents were recorded with an EPC-10 amplifier with Pulse 8.60 acquisition software and analyzed by Pulsefit 8.60 software (HEKA Electronik, Lambrecht, Germany). The data filtering and sampling frequencies were set at 2 and 10 kHz, respectively. After a whole-cell configuration was established, the holding potential was set at −70 mV; the cell was then subject to increasing depolarization (−70 to +70 mV with 10-mV increments) to obtain current–voltage relation curves, or to repetitive depolarizing pulses (−10 mV, 10-s intervals for Na^+ current measurement; +30 mV, 10-s intervals for K^+ current measurement) to record inhibitory effects by magnolol. All experiments were done at room temperature (~24 °C).

To obtain the activation curves, Na^+ currents were stimulated with increasing depolarization, and conductance (G) was calculated as:

$$G = I/V - \mathrm{Vr}$$

where $\mathrm{Vr} = (RT/zF)1n(Na_o/Na_i)$

V is the applied voltage, Vr is the reversal potential of Na^+, I is the current, R is the universal gas constant, T is the temperature, z is the ion valency (+1 in this case) and F is the Faraday constant. Na_o and Na_i are, respectively, bath and pipette Na^+ concentrations. The Boltzmann equation was used to fit the data for voltage-dependence of activation:

$$G/G\max = 1/\left\{1 + \exp\left[\left(V_{1/2} - V\right)/k\right]\right\}$$

where Gmax is the maximum conductance, $V_{1/2}$ is the half-maximal activation potential, and k the slope factor.

To construct the steady-state inactivation curve for Na^+ currents, a dual-pulse protocol was used: a test pulse step of −10 mV was preceded by a pre-pulse of 2 s of different potentials. For the steady-state inactivation curve for K^+ currents, the test pulse was set at +70 mV and the duration of pre-pulses was 10 s. In both cases, the test pulse currents (I) are normalized to the largest test pulse current (Imax) and plotted against the pre-pulse voltages. The Boltzmann equation was used to fit the data for steady-state inactivation:

$$I/I\max = 1/\left\{1 + \exp\left[\left(V - V_{1/2}\right)/k\right]\right\}$$

where $V_{1/2}$ is the half-maximal inactivation potential, and k the slope factor.

To obtain voltage-dependence of activation of Kv currents, voltage steps delivered in 10 mV increments from a holding potential of −70 mV were followed by a −40 mV step to trigger tail currents. Tail currents are normalized with the maximum tail current and then plotted against the voltage steps. Data are fit by the Boltzmann equation: $I/I\max = 1/\{1 + \exp[(V_{1/2} - V)/k]\}$, where $V_{1/2}$ is the half-maximal activation potential and k the slope factor.

Concentration–inhibition curves are fitted by the Hill equation:

$$I_{\mathrm{drug}}/I_{\mathrm{control}} = 1/\{1 + ([\mathrm{drug}]/\mathrm{IC}_{50})^n\}$$

where I_{drug} is the maximum current in the presence of magnolol, $I_{control}$ is the maximum current in the absence of magnolol, [drug] is the bath concentration of magnolol, IC_{50} is the concentration of drug which produces 50% inhibition of currents, and n is the Hill coefficient.

2.3. Statistical analysis

Data are presented as mean ± S.E.M. The unpaired or paired Student t test was used where appropriate to compare two groups. ANOVA was used to compare multiple groups, followed by the Tukey's HSD post-hoc test. A value of $P<0.05$ was considered to represent a significant difference.

3. Results

At a holding potential of −70 mV, addition of 30 μM magnolol strongly inhibited the Na^+ currents (tonic block) (Fig. 1A). Fig. 1B illustrates the concentration-dependent inhibition curve with an IC_{50} of 15 μM at a holding potential of −70 mV (solid circle). Note that at the latter holding potential, the Na^+ channels were partially inactivated (Fig. 3A). We also examined the concentration-dependent inhibition by magnolol at a holding potential of −100 mV, at which the Na^+ channels were not inactivated (fully available; Fig. 3A). At −100 mV holding potential, IC_{50} was 30 μM (Fig. 1B open circle). Therefore, magnolol was more potent when the Na^+ channels were partially inactivated.

We then examined if the magnolol inhibition was reversible. The inhibition by magnolol (30 μM) could be slowly and partially reversed by washout (Fig. 2). There was a 51 ± 19% recovery after washout ($n = 4$). The reason for the slow washout of magnolol is unknown. The same washout rate (25 ml/min) was used in our other studies to rapidly reverse drug inhibition of Na^+ and K^+ currents (Chou et al., 2009; Leung et al., 2010a).

Even when the extracellular bath solution contained 2 mM Ca^{2+}, voltage-gated Ca^{2+} currents in NG108-15 cells were barely detectable using the voltage-clamp method, while a very weak Ca^{2+} signal could be stimulated by 70 mM KCl using microfluorimetric imaging and fura-2 as dye (Leung et al., 2011). This suggests that voltage-gated Ca^{2+} channel expression in NG108-15 cells is very low, and channel activity runs down quickly once the whole-cell configuration is formed.

The effects of magnolol on Na^+ channel gating were next examined. In the presence of 30 μM magnolol, the steady-state inactivation curve left-shifted 18 mV ($V_{1/2} = -59.4 \pm 2.9$ mV and -78 ± 5.6 mV in the absence and presence of magnolol, respectively; $P<0.05$)

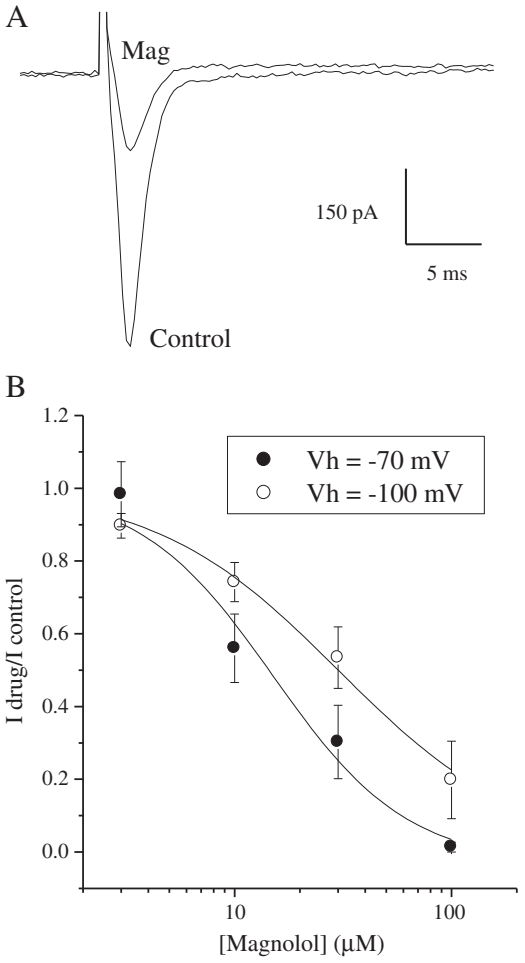

Fig. 1. Voltage-gated Na^+ current in NG108-15 cell was inhibited concentration-dependently by magnolol. (A) Representative traces of sodium currents triggered by −10 mV depolarization at a holding potential of −70 mV in the absence and presence of 30 μM magnolol. (B) Concentration–response curves of Na^+ current inhibition by magnolol at two holding potentials (−70 and −100 mV). Results represent mean ± S.E.M. from 3 t0 7 cells of each group.

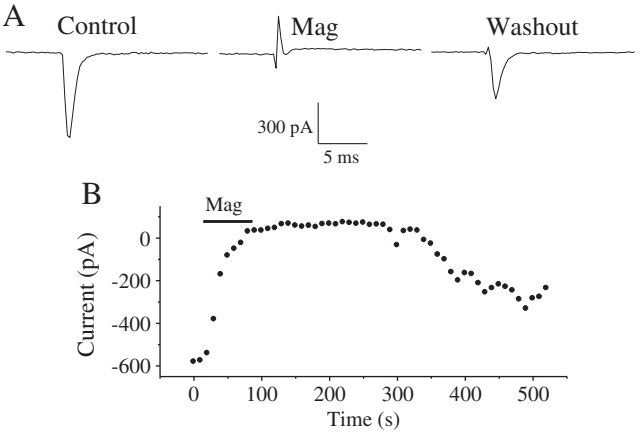

Fig. 2. Block of voltage-gated Na^+ currents in NG108-15 cells by magnolol was partially reversed upon washout. (A) Currents were triggered by −10 mV stimulations every 10 s during which 30 μM magnolol was added and then washed out (solution perfusion rate was 25 ml/min). The typical traces shown are currents before and after magnolol addition, and after washout of magnolol. (B) The peak currents are plotted against time. Similar results were obtained in 3 more experiments.

(Fig. 3A). Voltage-dependence of activation of Na^+ channels was not significantly affected by 30 μM magnolol (Fig. 3B).

Lidocaine blocks Na^+ channels with frequency-dependence, in such a manner that the cumulative block augments with stimulation frequency (Hille, 2001; Leung et al., 2010b). We examined if magnolol inhibited Na^+ currents with frequency-dependence. As shown in Fig. 4, current magnitude in the control was not significantly influenced by repeated stimulation (0.3–1.3 Hz; Fig. 4A–C). In the presence of 30 μM lidocaine, while inhibition did not enhance with consecutive stimulation at 0.3 Hz, increasing the stimulation rate to 0.6 and 1.3 Hz enhanced the cumulative block in a frequency-dependent fashion (Fig. 4A–C). However, the degree of inhibition by magnolol was not affected upon repeated stimulation at all the frequencies tested. Hence, the block by magnolol did not show frequency-dependence.

The effects of magnolol on Kv channels in NG108-15 cells were then examined. Addition of 100 μM magnolol substantially inhibited the Kv currents (Fig. 5A). Fig. 5B illustrates the concentration-dependent inhibition curve with an IC_{50} value of 20.8 μM. Fig. 5C

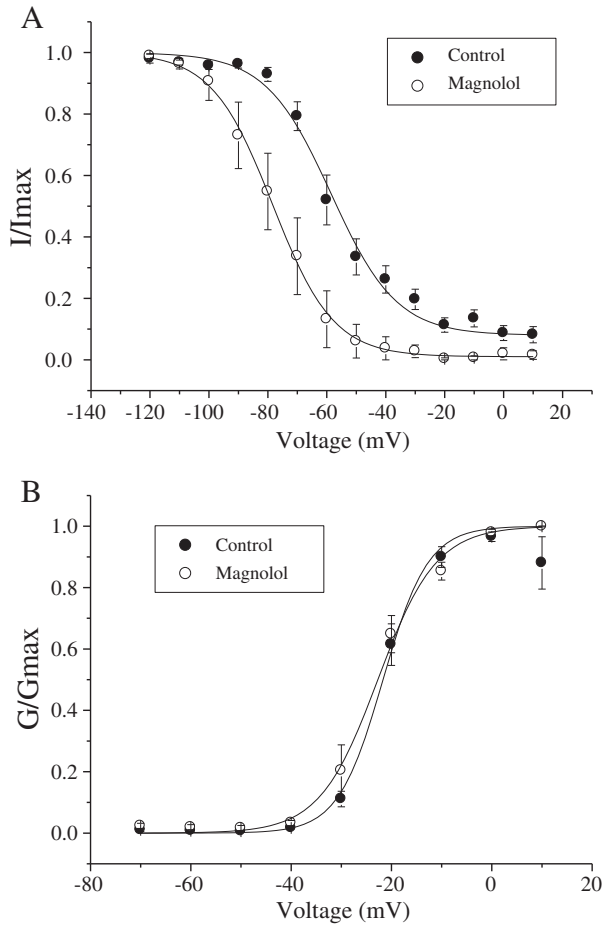

Fig. 3. Magnolol caused a left-shift in steady-state inactivation but did not affect voltage-dependence of activation of Na^+ currents in NG108-15 cells. (A) The steady-state inactivation protocol was performed in cells treated with and without 30 μM magnolol. A test pulse step of −10 mV was preceded by a pre-pulse of 2 s of different potentials. The test pulse currents are then normalized to the largest test pulse current and plotted against the pre-pulse voltages. The results are fitted by the Boltzmann equation. Results are mean ± S.E.M. from 4 to 7 cells of each group. (B) Voltage-dependence of activation: Na^+ currents were triggered by increasing depolarization (from a holding potential of −70 mV and then 10 mV increments), and conductance (G) is calculated as described in Materials and methods. Each conductance in the control group and the magnolol (30 μM)-treatment group is then normalized with the respective maximum conductance (Gmax) and then plotted against the applied depolarization voltages. The results are then fitted with the Boltzmann equation. Results are mean ± S.E.M. from 3 to 4 cells of each group.

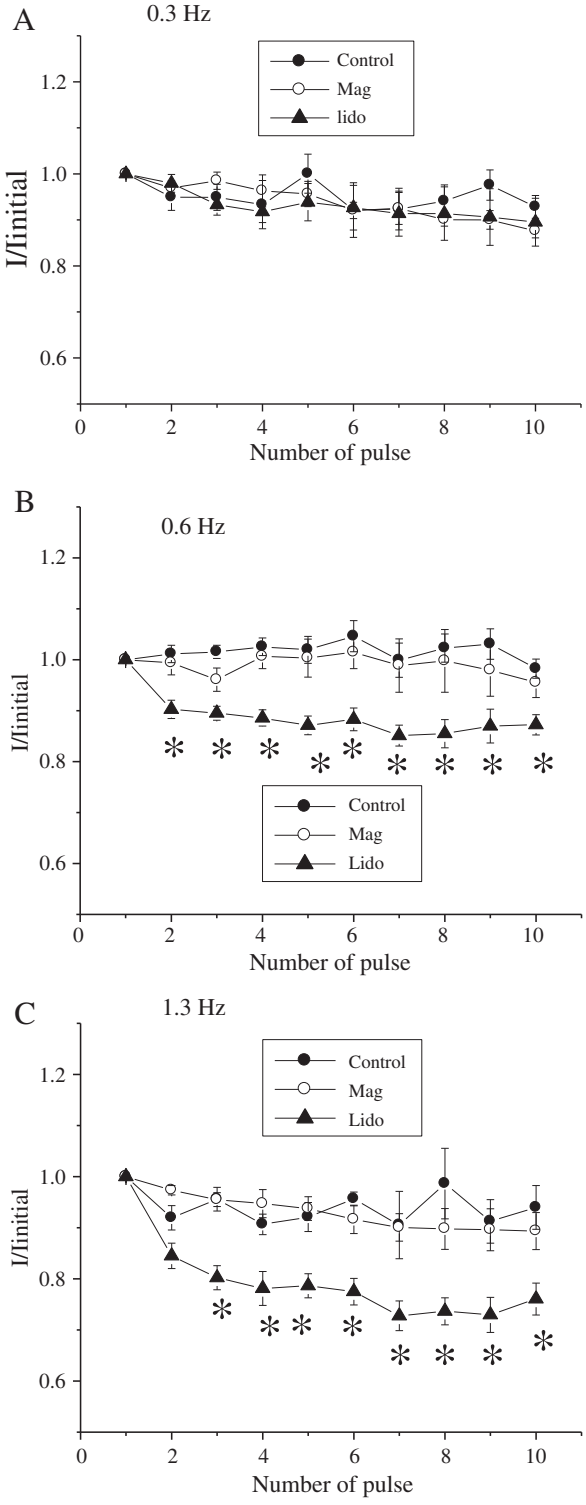

Fig. 4. Magnolol block of Na^+ currents in NG108-15 cells displayed no use-dependence. Cells were stimulated by −10 mV pulses at (A) 0.3 Hz, (B) 0.6 Hz and (C) 1.33 Hz in the absence or presence of 30 μM magnolol or 30 μM lidocaine. The maximum current amplitudes of the second to tenth pulses (I) are normalized with the maximum current amplitudes of the first pulse ($I_{initial}$) and then plotted against the number of pulse. * indicates significant difference ($P<0.05$) from the control. Results are mean ± S.E.M. from 4 to 7 cells of each group.

shows that inhibition of Kv currents by magnolol (30 μM) was largely reversible (inhibition was 42 ± 4%, and recovery after washout reached 96 ± 7%; $n=4$). In the presence of 20 μM magnolol, the steady-state inactivation curve shifts to the left by 20 mV ($V_{1/2}$ = −18.9 ± 0.9 mV and −39.3 ± 3.5 mV in the absence and presence of magnolol, respectively; $P<0.05$) (Fig. 6A). However, magnolol (20 μM) did not alter the voltage-dependence of activation (Fig. 6B).

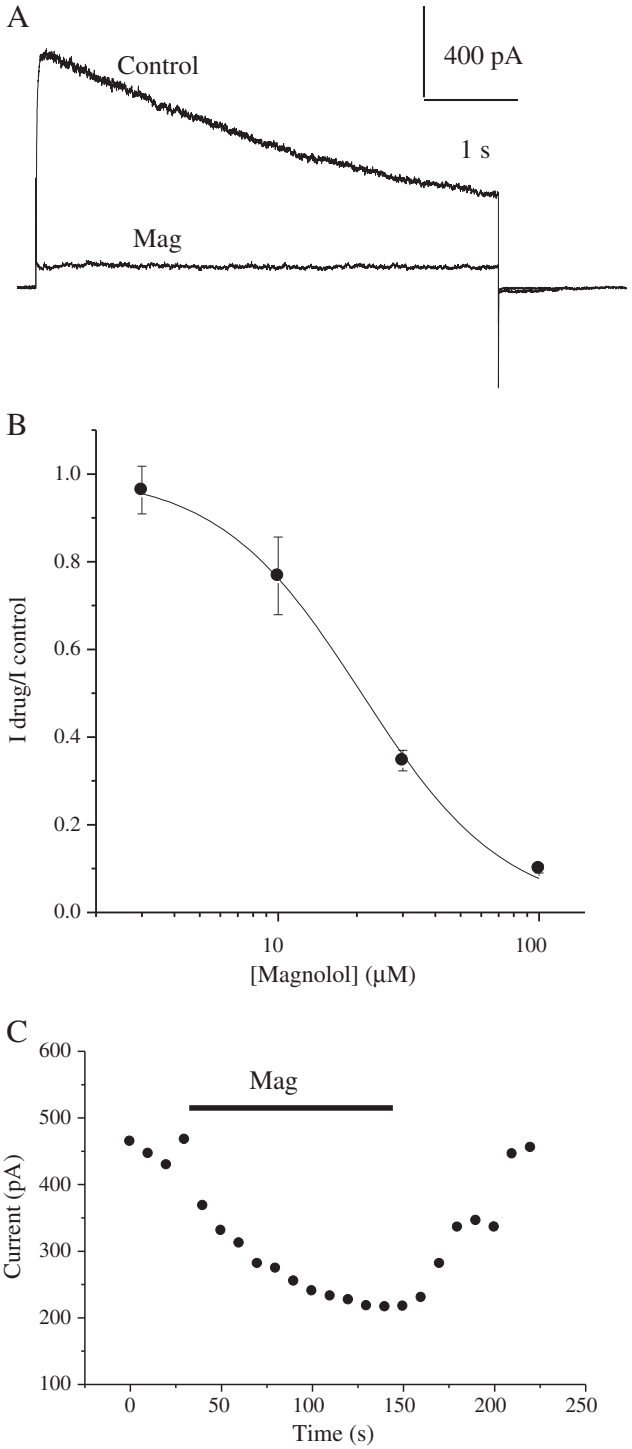

Fig. 5. Magnolol inhibited voltage-gated K^+ currents in NG108-15 cells. (A) Outward K^+ currents were triggered by +30 mV pulses every 10 s and magnolol (100 μM) was added to the bath. The traces show the currents obtained before magnolol and after the inhibitory effect of magnolol has reached a steady-state. (B) Concentration–response curve of magnolol inhibition. Results are mean ± S.E.M. from 3 to 4 cells of each group. (C) Inhibition of Kv currents by 30 μM magnolol could be reversed by washout. Currents were triggered by +30 mV stimulations every 10 s during which 30 μM magnolol was added and then washed out (solution perfusion rate was 25 ml/min). The end-of-pulse currents are plotted against time. Similar results were obtained in 3 more experiments.

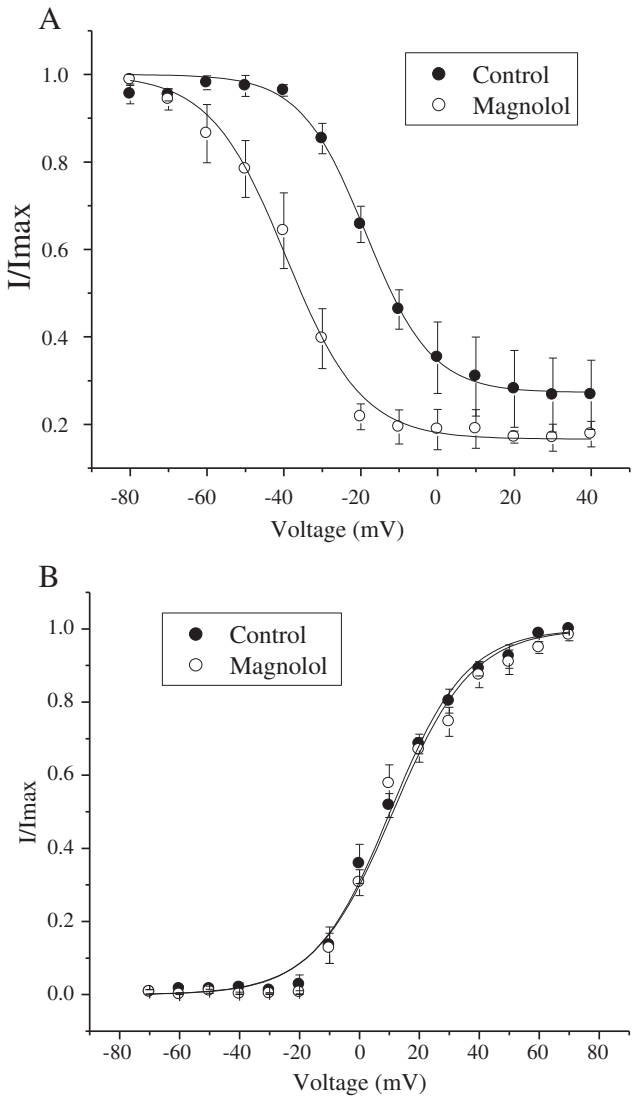

Fig. 6. Magnolol caused a left-shift in the steady-state inactivation curve of Kv currents in NG108-15 cells. (A) The steady-state inactivation protocol was performed in cells treated with and without 20 μM magnolol. A test pulse step of +70 mV was preceded by a pre-pulse of 10 s of different potentials. The test pulse currents are then normalized to the largest test pulse current and plotted against the pre-pulse voltages. The results are fitted by the Boltzmann equation. Results are mean ± S.E.M. from 3 to 4 cells of each group. (B) Voltage-dependence of activation: voltage steps delivered in 10 mV increments from a holding potential of −70 mV were followed by a −40 mV step to trigger tail currents. Normalized tail currents are then plotted against the various voltage steps. The curves are fitted by the Boltzmann equation. Results are mean ± S.E.M. from 5 cells of each group.

4. Discussion

Although the beneficial effects of magnolol on neuronal tissues have been well known in *in vitro* and *in vivo* studies, very limited information is available on how magnolol directly affects neuronal ion channels. A previous study showed, using fluorimetric assay, that magnolol could inhibit Ca^{2+} influx triggered by glutamate and KCl-induced depolarization, implicating that magnolol may block glutamate receptor-channels and voltage-gated Ca^{2+} channels (Lin et al., 2005). Given that VGSC and Kv channels directly control neuronal excitability, it would be of interest to examine the effects of magnolol on these channels. The present work showed for the first time that magnolol inhibited both VGSC and Kv channels.

The inhibitory effect of magnolol on VGSC was accompanied with a left-shift of the steady-state inactivation curve, indicating that the availability of VGSC was reduced upon binding with magnolol. However, the voltage-dependence of activation was not affected, indicating that magnolol did not affect activation gating. The left-shift in the steady-state inactivation curve suggests that, in the presence of magnolol, inactivation of VGSC was intensified. This is consistent with the state-dependence of magnolol block (Fig. 1B). These data suggest that magnolol binds to the inactivated state of VGSC with higher affinity. Kv channel availability was also reduced by magnolol treatment, as the latter caused a left-shift in the steady-state inactivation curve (Fig. 6A).

Local anesthetics, such as lidocaine, have been demonstrated to display two modes of block, namely, tonic block (or closed channel block) and phasic block (or open channel block) (Hille, 2001). The former block does not require channel opening, while the latter block only proceeds when the cytoplasmic activation gate opens to let the drug gain access to the internal cavity of the VGSC. In this open channel block, the more frequently the channel opens, the more the cumulative block. While it can be shown that lidocaine expectedly displayed this use-dependence or frequency-dependence of open channel block, magnolol block was not enhanced at all by increasing the frequency of stimulation (Fig. 4). Thus, magnolol block was not frequency-dependent, implying it is unlikely that magnolol has to gain access to the internal vestibule in order to block.

Upon washout of magnolol, the recovery of VGSC block was slow and only partial (Fig. 2) while recovery of Kv channel block was fast and almost complete (Fig. 5C). The cause for these differences in the rate and extent of recovery from block between the VGSC and Kv channels is unknown and remains to be determined.

Block of VGSC by magnolol may in part explain the reported analgesic effect of this drug in mice (Lin et al., 2007, 2009). Na^+ channel blockade is believed to be one of the mechanisms leading to the anxiolytic effects of drugs such as lamotrigine, carbamazepine and riluzole (Bourin et al., 2009; Mirza et al., 2005). The anxiolytic property of magnolol (Maruyama et al., 1998) may be in part attributed to the inhibition of Na^+ currents by this herbal compound.

Since cytosolic K^+ inhibits an array of pro-apototic nucleases and caspases, it has been known that excessive K^+ efflux due to Kv channel overexpression is a cause for neuronal apoptotic death (Yu, 2003). Subtype members from Kv1 to Kv4 subfamilies have been implicated in apoptosis in a variety of neurons; blockade or inhibition of expression of Kv channels could prevent or alleviate neuronal apoptosis (for a review see Leung, 2010). The Kv subfamily members expressed in NG108-15 cells have been identified to be Kv1.2 and Kv3.1 (Yokoyama et al., 1993). We reported here that magnolol could strongly inhibit Kv channel currents; this property may also render this drug a potential neuroprotective agent (Leung, 2010).

Magnolol has been reported to have Ca^{2+} antagonistic effects in vascular smooth muscle (Teng et al., 1990). Thus, magnolol may have antihypertensive effects. Other works have also shown that magnolol blocks voltage-gated Ca^{2+} entry in smooth muscle cells of other tissues, such as porcine trachea (Ko et al., 2003), rat uterus (Lu et al., 2003) and guinea pig colon (Bian et al., 2006). Therefore magnolol may have potential therapeutic applications in asthma, uterine and intestinal spasm.

It is noted that magnolol has a stimulatory effect on the large-conductance Ca^{2+}-activated K^+ channels in smooth muscle cells of human trachea (Wu et al., 2002). Magnolol enhances channel open probability and also causes a left shift in the activation curve. Large-conductance Ca^{2+}-activated K^+ channels are activated by membrane depolarization and micromolar range of cytosolic Ca^{2+}; and by providing K^+ efflux these channels serve to dampen cellular excitability (Salkoff et al., 2006). Magnolol, because of its ability to activate large-conductance Ca^{2+}-activated K^+ channels in trachea, may be a potential anti-asthmic agent.

Given that magnolol affects multiple receptors and channels such as GABA receptors (Chen et al., 2011), NMDA receptors (Lin et al.,

2005), voltage-gated Ca^{2+} channels (Ko et al., 2003; Lin et al., 2005; Lu et al., 2003), large-conductance Ca^{2+}-activated K^+ channels (Wu et al., 2002), VGSC and Kv channels (the present work), the pharmacological effects of magnolol are considered to lack specificity. Therefore, the possibility that magnolol acts by directly modifying plasma membrane structure should not be ruled out.

5. Conclusion

This report showed that magnolol inhibited VGSC and Kv channels in NG108-15 cells. Magnolol also altered the gatings of these channels. These properties may in part account for the previously reported effects of magnolol on neural tissues.

Acknowledgments

We would like to thank China Medical University, Taiwan, and the Taiwan National Science Council for research funds to YML and KLW (CMU99-S-16; CMU100-S-24; DMR-99-097; NSC 97-2320-B-039-029-MY3).

The authors declare no conflict of interests.

References

Bian, Z.X., Zhang, G.S., Wong, K.L., Hu, X.G., Liu, L., Yang, Z., Li, M., 2006. Inhibitory effects of magnolol on distal colon of guinea pig in vitro. Biol. Pharm. Bull. 29, 790–795.

Bourin, M., Chenu, F., Hascoet, M., 2009. The role of sodium channels in the mechanism of action of antidepressants and mood stabilizers. Curr. Drug Targets 10, 1052–1060.

Chang, C.P., Hsu, Y.C., Lin, M.T., 2003. Magnolol protects against cerebral ischaemic injury of rat heatstroke. Clin. Exp. Pharmacol. Physiol. 30, 387–392.

Chen, L.C., Liu, Y.C., Liang, Y.C., Ho, Y.S., Lee, W.S., 2009. Magnolol inhibits human glioblastoma cell proliferation through upregulation of p21/Cip1. J. Agric. Food Chem. 57, 7331–7337.

Chen, C., Tan, R., Qu, W., Wu, Z., Wang, Y., Urade, Y., Huang, Z., 2011. Magnolol, a major bioactive constituent of the bark of Magnolia officinalis, exerts anti-epileptic effects via GABA-benzodiazepine receptor complex in mice. Br. J. Pharmacol. 164, 1534–1546.

Chou, C.H., Gong, C.L., Chao, C.C., Lin, C.H., Kwan, C.Y., Hsieh, C.L., Leung, Y.M., 2009. Rhynchophylline from Uncaria rhynchophylla functionally turns delayed rectifiers into A-Type K+ channels. J. Nat. Prod. 72, 830–834.

Hamprecht, B., Glaser, T., Reiser, G., Bayer, E., Propst, F., 1985. Culture and characteristics of hormone-responsive neuroblastoma x glioma hybrid cells. Methods Enzymol. 109, 316–341.

Hille, B., 2001. Ion Channels of Excitable Membranes. Sinauer, Sunderland, Mass.

Huang, S.H., Chen, Y., Tung, P.Y., Wu, J.C., Chen, K.H., Wu, J.M., Wang, S.M., 2007. Mechanisms for the magnolol-induced cell death of CGTH W-2 thyroid carcinoma cells. J. Cell. Biochem. 101, 1011–1022.

Ko, C.H., Chen, H.H., Lin, Y.R., Chan, M.H., 2003. Inhibition of smooth muscle contraction by magnolol and honokiol in porcine trachea. Planta Med. 69, 532–536.

Lee, M.M., Hseih, M.T., Kuo, J.S., Yeh, F.T., Huang, H.M., 1998. Magnolol protects cortical neuronal cells from chemical hypoxia in rats. Neuroreport 9, 3451–3456.

Lee, S.J., Cho, Y.H., Park, K., Kim, E.J., Jung, K.H., Park, S.S., Kim, W.J., Moon, S.K., 2008. Magnolol elicits activation of the extracellular signal-regulated kinase pathway by inducing p27KIP1-mediated G2/M-phase cell cycle arrest in human urinary bladder cancer 5637 cells. Biochem. Pharmacol. 75, 2289–2300.

Leung, Y.M., 2010. Voltage-gated K+ channel modulators as neuroprotective agents. Life Sci. 86, 775–780.

Leung, Y.M., Kuo, Y.H., Chao, C.C., Tsou, Y.H., Chou, C.H., Lin, C.H., Wong, K.L., 2010a. Osthol is a use-dependent blocker of voltage-gated Na+ channels in mouse neuroblastoma N2A cells. Planta Med. 76, 34–40.

Leung, Y.M., Wu, B.T., Chen, Y.C., Hung, C.H., Chen, Y.W., 2010b. Diphenidol inhibited sodium currents and produced spinal anesthesia. Neuropharmacology 58, 1147–1152.

Leung, Y.M., Huang, C.F., Chao, C.C., Lu, D.Y., Kuo, C.S., Cheng, T.H., Chang, L.Y., Chou, C.H., 2011. Voltage-gated K+ channels play a role in cAMP-stimulated neuritogenesis in mouse neuroblastoma N2A cells. J. Cell. Physiol. 226, 1090–1098.

Lin, Y.R., Chen, H.H., Ko, C.H., Chan, M.H., 2005. Differential inhibitory effects of honokiol and magnolol on excitatory amino acid-evoked cation signals and NMDA-induced seizures. Neuropharmacology 49, 542–550.

Lin, Y.R., Chen, H.H., Ko, C.H., Chan, M.H., 2006. Neuroprotective activity of honokiol and magnolol in cerebellar granule cell damage. Eur. J. Pharmacol. 537, 64–69.

Lin, Y.R., Chen, H.H., Ko, C.H., Chan, M.H., 2007. Effects of honokiol and magnolol on acute and inflammatory pain models in mice. Life Sci. 81, 1071–1078.

Lin, Y.R., Chen, H.H., Lin, Y.C., Ko, C.H., Chan, M.H., 2009. Antinociceptive actions of honokiol and magnolol on glutamatergic and inflammatory pain. J. Biomed. Sci. 16, 94.

Lu, Y.C., Chen, H.H., Ko, C.H., Lin, Y.R., Chan, M.H., 2003. The mechanism of honokiol-induced and magnolol-induced inhibition on muscle contraction and Ca2+ mobilization in rat uterus. Naunyn Schmiedebergs Arch. Pharmacol. 368, 262–269.

Mainardi, T., Kapoor, S., Bielory, L., 2009. Complementary and alternative medicine: herbs, phytochemicals and vitamins and their immunologic effects. J. Allergy Clin. Immunol. 123, 283–294.

Maruyama, Y., Kuribara, H., Morita, M., Yuzurihara, M., Weintraub, S.T., 1998. Identification of magnolol and honokiol as anxiolytic agents in extracts of saiboku-to, an oriental herbal medicine. J. Nat. Prod. 61, 135–138.

Matsui, N., Nakashima, H., Ushio, Y., Tada, T., Shirono, A., Fukuyama, Y., Nakade, K., Zhai, H., Yasui, Y., Fukuishi, N., Akagi, R., Akagi, M., 2005. Neurotrophic effect of magnolol in the hippocampal CA1 region of senescence-accelerated mice (SAMP1). Biol. Pharm. Bull. 28, 1762–1765.

Matsui, N., Takahashi, K., Takeichi, M., Kuroshita, T., Noguchi, K., Yamazaki, K., Tagashira, H., Tsutsui, K., Okada, H., Kido, Y., Yasui, Y., Fukuishi, N., Fukuyama, Y., Akagi, M., 2009. Magnolol and honokiol prevent learning and memory impairment and cholinergic deficit in SAMP8 mice. Brain Res. 1305, 108–117.

Mirza, N.R., Bright, J.L., Stanhope, K.J., Wyatt, A., Harrington, N.R., 2005. Lamotrigine has an anxiolytic-like profile in the rat conditioned emotional response test of anxiety: a potential role for sodium channels? Psychopharmacology (Berl) 180, 159–168.

Salkoff, L., Butler, A., Ferreira, G., Santi, C., Wei, A., 2006. High-conductance potassium channels of the SLO family. Nat. Rev. Neurosci. 7, 921–931.

Shen, J.L., Man, K.M., Huang, P.H., Chen, W.C., Chen, D.C., Cheng, Y.W., Liu, P.L., Chou, M.C., Chen, Y.H., 2010. Honokiol and magnolol as multifunctional antioxidative molecules for dermatologic disorders. Molecules 15, 6452–6465.

Teng, C.M., Yu, S.M., Chen, C.C., Huang, Y.L., Huang, T.F., 1990. EDRF-release and Ca+(+)-channel blockade by magnolol, an antiplatelet agent isolated from Chinese herb Magnolia officinalis, in rat thoracic aorta. Life Sci. 47, 1153–1161.

Wu, S.N., Chen, C.C., Li, H.F., Lo, Y.K., Chen, S.A., Chiang, H.T., 2002. Stimulation of the BK(Ca) channel in cultured smooth muscle cells of human trachea by magnolol. Thorax 57, 67–74.

Xu, Q., Yi, L.T., Pan, Y., Wang, X., Li, Y.C., Li, J.M., Wang, C.P., Kong, L.D., 2008. Antidepressant-like effects of the mixture of honokiol and magnolol from the barks of *Magnolia officinalis* in stressed rodents. Prog. Neuropsychopharmacol. Biol. Psychiatry 32, 715–725.

Yokoyama, S., Kawamura, T., Ito, Y., Hoshi, N., Enomoto, K., Higashida, H., 1993. Potassium channels cloned from NG108-15 neuroblastoma-glioma hybrid cells. Functional expression in *Xenopus* oocytes and mammalian fibroblast cells. Ann. N. Y. Acad. Sci. 707, 60–73.

Yu, S.P., 2003. Regulation and critical role of potassium homeostasis in apoptosis. Prog. Neurobiol. 70, 363–386.